Enhanced decolorization of azo dye solution by cadmium sulfide/multi-walled carbon nanotubes/polymer composite in combination with hydrogen peroxide under simulated solar light irradiation

H.-Y. Zhu[a], J. Yao[a], R. Jiang[a,b,*], Y.-Q. Fu[a], Y.-H. Wu[a], G.-M. Zeng[c,**]

[a]Department of Environmental Engineering, College of Life Science, Taizhou University, Taizhou, Zhejiang 318000, PR China
[b]Department of Chemistry, Zhejiang University, Hangzhou, Zhejiang 310027, PR China
[c]Key Laboratory of Environmental Biology and Pollution Control (Hunan University), Ministry of Education, Changsha, Hunan 410082, PR China

Abstract

Cadmium sulfide/multi-walled carbon nanotubes/polymer nanocomposite (CdS/MWCNTs/polymer) was fabricated via a facile precipitation process by depositing nanocrystalline CdS on carbon nanotubes/crosslinked chitosan nanocomposite and characterized by X-ray diffraction (XRD) and transmission electron microscope (TEM). Under simulated solar light irradiation, a combination of CdS/MWCNTs/polymer and H_2O_2 was found to be highly efficient for photocatalytic decolorization of a soluble azo dye, methyl orange (MO), even at neutral pH values. 99.9% of MO solution was successfully decolorized after 90 min under simulated solar light irradiation with 15 mg L^{-1} of initial MO concentration, 1.0 mM of H_2O_2 concentration and 0.70 g L^{-1} of photocatalyst dosage. Experimental results also indicated that the photocatalytic decolorization of methyl orange solution was strongly influenced by operational parameters and followed a simplified Langmuir–Hinshelwood (L–H) kinetic model with high R^2 values. When the CdS/MWCNTs/polymer–H_2O_2 system was reused for the 5th time, the decolorization efficiency was still about 88.0% after 90 min under simulated solar light irradiation. As a result, the CdS/MWCNTs/polymer–H_2O_2 will potentially provide cheaper and cleaner means for the effective treatment of dyeing effluents since it increased substantially the efficiency of dye decolorization and could take full advantage of economical solar light.
© 2013 Elsevier Ltd and Techna Group S.r.l. All rights reserved.

Keywords: Photocatalytic decolorization; Methyl orange; CdS; Carbon nanotubes; H_2O_2

1. Introduction

Wastewater effluents discharged from textile, printing, pulp, tanneries and leather industries have emerged as a focus of environmental remediation efforts [1]. It is estimated that 30,000–150,000 t of synthetic dyes are released into open waters [2]. These synthetic dyes are generally stable compounds, which are difficult to be destroyed or removed by common biological treatment [3]. What is more, these colored effluents are often considered to be highly toxic to aquatic biota [4,5]. All kinds of physical–chemical methods including photocatalysis and adsorption have been developed to treat wastewater effluents containing dyes [6,7].

It is well-known that heterogeneous photocatalysis based photocatalyst is one of the most successful and convenient methods for the removal of undesirable organic pollutants existing in wastewater [2]. Recent studies have proven that photocatalysis is an effective method to treat containing-dye effluents [7–9]. From both viewpoint of environment protection and energy utilization, visible light-driven photocatalysis for organic pollution treatment has attracted great interest in recent years since UV light accounts for only a small fraction (5%) of the sun's energy compared to visible region (45%) [10,11]. Therefore, many attempts have been made to improve

*Correspondence to: No.1139, Municipal Government Avenue, Taizhou City, Zhejiang Province 318000, PR China. Tel.: +86 0158 6763 6396; fax: +86 0576 8866 0388.
**Corresponding author. Tel.: +86 731 8822 829; fax: +86 731 8823 701.
E-mail addresses: jiangru0576@163.com (R. Jiang), zgming@hnu.cn (G.-M. Zeng).

the utilization of visible light during photocatalysis [2]. Cadmium sulfide (CdS), as an n-type semiconductor with a relatively narrow band gap of approximately 2.42 eV (512 nm), is one of the most studied semiconductors [10–14]. CdS is also used as a solar light-driven photocatalyst to treat these colored effluents by heterogeneous photocatalysis [8,15,16]. In addition, heterogeneous photocatalytic reactions primarily take place on the surface of photocatalyst [17]. Therefore, the effective adsorption of objective pollutants on the surface of photocatalyst was favorable for pollutant degradation by $^\bullet OH$, which was confirmed by electron spin resonance spin-trapping technique [18]. Some studies have also verified that carbon nanotubes (CNTs) are a promising adsorption material for pollutants and support for photocatalyst due to their extraordinary mechanical strength and relatively large specific area [18–21]. Recently, CdS nanoparticles have been successfully attached on carbon nanotubes *in situ* [21–23]. The conductive structure of CNTs may facilitate fast separation of photo-generated electron/hole (e^-/h^+) pairs at the composite photocatalyst interface, leading to enhanced rates of photocatalytic oxidation [24].

In order to remove organic pollutants more effectively, the combination of heterogeneous photocatalysis with some powerful oxidants such as O_3 and H_2O_2 can be a promising alternative [17,18,25]. The introduction of H_2O_2, as an efficient electron scavenger and a source of hydroxy radical ($^\bullet OH$) with high oxidizing ability (oxidation potential is 2.8 eV), can prevent the recombination of e^-/h^+ pairs and lead to an effectively photocatalytic decolorization of organic dye pollutants [11]. The reaction rate constant for the combined system of semiconductor photocatalyst and H_2O_2 was always much higher than that for an individual system [25,26]. Therefore, the combination can effectively increase the rate of photocatalytic decolorization of dye pollutant and shorten treatment time. However, few studies have been reported on a full investigation of the efficient simulated solar light-induced photocatalytic decolorization of azo dye by CdS/multi-walled carbon nanotubes/polymer nanocomposite (CdS/MWCNTs/polymer) in the presence of H_2O_2 (CdS/MWCNTs/polymer–H_2O_2 system in short).

In this study, a heterogeneous photocatalytic process (CdS/MWCNTs/polymer–H_2O_2 system) was evaluated to decolorize dyeing effluents. Effects of key operating variables, such as pH, hydrogen peroxide concentration, and initial dye concentration on decolorization were studied. The present investigation may provide a practical and cost-effective method for effective treatment of wastewater effluents containing dyes.
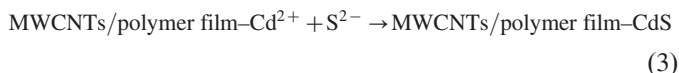
2. Experimental

2.1. Materials

Multi-walled carbon nanotubes (MWCNTs, OD × ID × length: 8 nm × 2–3 nm × 30 μm, purity > 95 wt%) were purchased from Chengdu Organic Chemistry Co. Ltd., Chinese Academy of Sciences (Chengdu, China) and used without further treatment. Methyl orange (MO) was purchased from Yongjia Fine Chemical Factory (Wenzhou, China). Chitosan

obtained from Yuhuan Ocean Biochemistry Co. (Taizhou, China) was used as a polymer matrix. Its deacetylation degree (DD) and weight average molecular weight was 91% and 2.1×10^5, respectively. $CdCl_2$ and $(NH_2)_2CS$ were used as raw materials for CdS nanocrystalline. Other chemicals used in this study such as glutaraldehyde, NaOH, NaCl, $NaNO_3$, Na_2SO_4, Na_2CO_3, and Na_3PO_4 were of analytical reagent grade from Shanghai Chemical Reagent Co., Ltd (Shanghai, China).

2.2. Preparation and characterization of CdS/MWCNTs/polymer

With continuous ultrasonic stirring, 0.912 g of $CdCl_2$ and 0.100 g of MWCNTs were mixed in 100 mL of 2% (w/v) chitosan acetate solution for 30 h to form a colloidal system. Subsequently, the homogeneous colloidal system was cast evenly on clean glass plates. After drying under ambient temperature, glass plates with thin films were immersed into 0.2 mol L^{-1} of NaOH solution and thin composite films were peeled off from glass plates. The fresh composite thin films were dipped into a 0.2 mol L^{-1} of thiocarbamide aqueous solution (20 mL) in a constant temperature water bath at 70 ± 0.2 °C for 30 min. 0.5 mol L^{-1} of NaOH solution (40 mL) was added dropwise to the reaction system to adjust pH to 11 in order to form CdS nanocrystalline slowly in the composite films. In an alkali medium, hydrolysis reactions of sulfocarbamide took place at 70 °C as described in Eqs. (1) and (2). Cd^{2+} ions embedded in or on MWCNTs/polymer films reacted slowly with S^{2-} anions to form CdS nanocrystalline according to Eq. (3). In order to enhance the acid resistance, the composite films were subsequently crosslinked by immersing into a 100 mL of 0.5% (v/v) glutaraldehyde solution for 30 min. Then the brown composite thin films were washed using absolute ethanol and double distilled water for 3–4 times, respectively, in order to remove excess glutaraldehyde. Finally, the products (CdS/MWCNTs/polymer) were dried at 60 °C under atmospheric condition and the dry composite films were cut into flakelets (0.5 cm × 0.5 cm).

$$(NH_2)_2CS + OH^- \rightarrow CH_2N_2 + H_2O + HS^- \tag{1}$$

$$HS^- + OH^- \rightarrow S^{2-} + H_2O \tag{2}$$

$$\text{MWCNTs/polymer film–}Cd^{2+} + S^{2-} \rightarrow \text{MWCNTs/polymer film–CdS} \tag{3}$$

The MWCNTs/polymer films were prepared using the same procedure, but without the addition of $CdCl_2$. The crystalline structure of MWCNTs/polymer films and CdS/MWCNTs/polymer were analyzed using a D8 Advance X-ray diffractometer (Bruker, Germany) with Cu Kα radiation (1.5406 A). The accelerating voltage and the applied current were 40 kV and 30 mA, respectively. Morphology and nanocrystal size of materials were characterized by using a JEOL 2010 FET transmission electron microscope (Tokyo, Japan).

2.3. Photocatalytic experiments and measurement of dye concentration

A 300 W xenon lamp (PLS-SXE300, Beijing Trusttech Co. Ltd, China) was used as a simulated solar light source. The wavelength of simulated solar light irradiation was in the range from 300 nm to 1100 nm. According to a technical report of PLS-SXE300, UV output (< 390 nm) was about 5.2% of irradiation energy while simulated solar light output (390 nm–770 nm) was about 39.2%. A 100 mL of MO aqueous solution and 0.07 g of CdS/MWCNTs/polymer composite films were added into photocatalytic reactor. Before simulated solar light irradiation, H_2O_2 were also added into the dye solution to obtain final concentration of H_2O_2 in solution in a range of 0–1.5 mM. During photocatalytic decolorization, the reaction system was stirred with air at a flow rate of 100 mL min^{-1}. The concentrations of MO were measured with a UV–vis spectrophotometer (Varian Cary 50) in the range of 200–700 nm, and the absorbance at 463.0 nm corresponded to the maximal absorption of MO solution was recorded. Effects of variables such as photocatalyst dosage (0.1–0.9 g L^{-1}) and H_2O_2 concentration (0–1.5 mM), initial MO concentration (5–30 mg L^{-1}), pH (2.0–12) and temperature (20–50 °C) were studied. The experiments were conducted by changing one variable at a period of time while keeping other parameters constant.

3. Results and discussion

3.1. Characterization of material

The crystal phase structures of CdS/MWCNTs/polymer films and MWCNTs/polymer films were characterized by XRD measurements and corresponding results are shown in Fig. 1. The patterns of MWCNTs/polymer exhibited the characteristic peak of polymer (chitosan) at $2\theta = 19.78°$, which coincided with the pattern of the tendon hydrate polymorph of chitosan reported previously [27,28]. As for the weak peak at
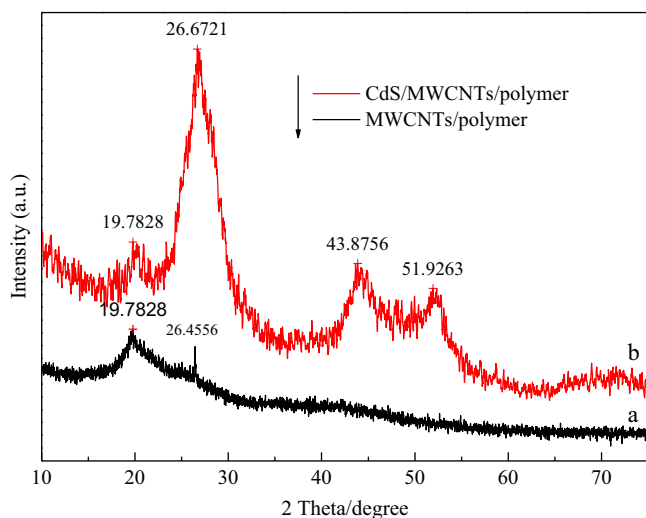

Fig. 1. XRD patterns of MWCNTs/polymer (a) and CdS/MWCNTs/polymer (b).

26.46° in the pattern of MWCNTs/polymer, it was assigned to (0 0 2) planes of the MWCNTs [29]. Compared with the XRD pattern of MWCNTs/polymer, the additional peaks at 2θ values of 26.67°, 43.88° and 51.93° in the XRD pattern of CdS/MWCNTs/polymer, correspond to the crystal planes of (1 1 1), (2 2 0) and (3 1 1) of the crystalline cubic CdS (JCPDS 75-1546), respectively [23], which indicated that the cubic CdS nanocrystal structure was formed successfully in the MWCNTs/polymer composite matrix.

The microstructures and nanocrystal size were observed by TEM and the results showed in Fig. 2. It can also be observed that raw MWCNT is mostly straight and smooth (Fig. 2a). Obviously, nanocrystals (CdS) of 25–30 nm diameters are attached the surface of MWCNTs/chitosan composite (Fig. 2b).

3.2. Effect of different processes on decolorization of MO solution

In order to study the effect of the photocatalyst and H_2O_2 on dye decolorization, MO solutions were exposed under four different processes, that is direct photolysis under simulated solar light irradiation, H_2O_2 in dark, photocatalytic decolorization by CdS/MWCNTs/polymer under simulated solar light irradiation, and photocatalytic decolorization by CdS/MWCNTs/polymer–H_2O_2 system under simulated solar light irradiation. The results are shown in Fig. 3. Obviously, almost no decolorization of MO solution was observed with only H_2O_2 in dark (Fig. 3a). Under simulated solar light irradiation without any additive, the removal rate of MO solution was about 16.5% after 90 min (Fig. 3b). About 72.5% of MO was successfully decolorized after 90 min in the case of 0.7 g L^{-1} CdS/MWCNTs/polymer and in the absence of H_2O_2 (Fig. 3c), implying that CdS/MWCNTs/polymer exhibited high visible light photocatalytic activity. However, the efficiency was still relatively low for practical application in appropriate time. When a small amount of H_2O_2 (1.0 mM) was added into the reaction system, it could be seen from the Fig. 3d that 99.9% of the azo dye was removed after 90 min irradiation while 72.8% in the absence of hydrogen peroxide (Fig. 3c). Obviously, nearly complete MO decolorization occurred after 90 min of simulated solar light irradiation, showing the beneficial effect of H_2O_2 addition on the photocatalytic decolorization. Therefore, significantly enhanced decolorization of MO solution in CdS/MWCNTs/polymer–H_2O_2 combination system was observed. As a result, the following experiments were carried out in the presence of hydrogen peroxide.

Highly efficient photocatalytic decolorization in CdS/MWCNTs/polymer–H_2O_2 system can be proven by monitoring the change in absorption spectra of MO solution as a function of irradiation time and the corresponding result is shown in Fig. 4. The chromophore of azo dyes such as MO resulted in an obvious absorption in the visible region while aromatic rings such as naphthalene and benzene rings in the UV region [12,30]. As observed from raw spectrum of MO solution (Fig. 4), primary absorption peaks of the dye solution
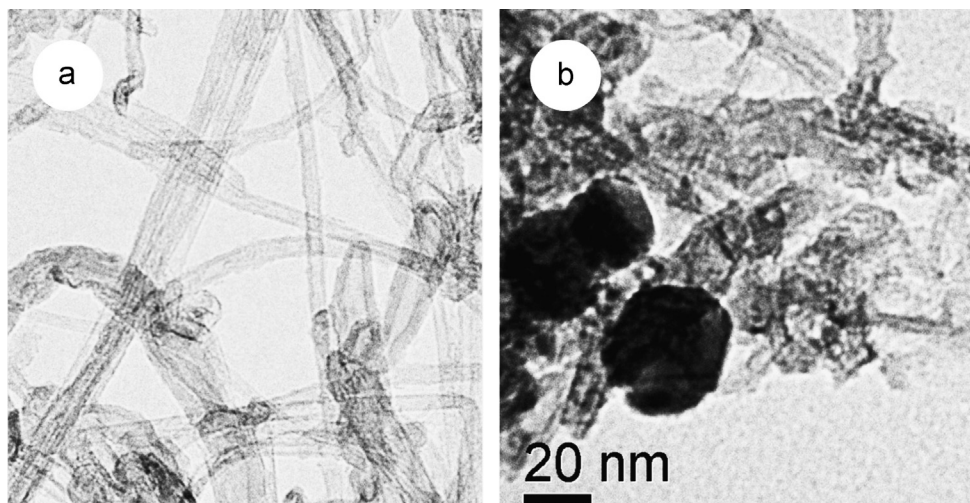
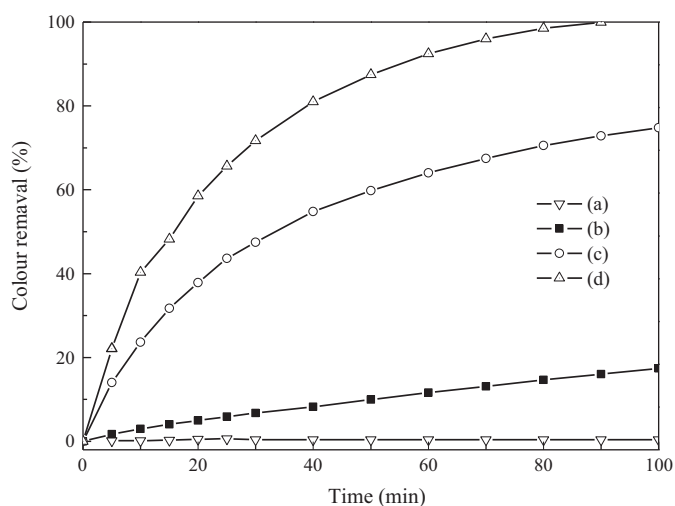Fig. 2. Typical TEM images of MWNTCS (a) and CdS/MWCNTs/polymer (b).

Fig. 3. Comparison of four different processes for decolorization of MO solutions: (a) H_2O_2 in dark, (b) direct photolysis under simulated solar light irradiation, (c) photocatalytic decolorization on CdS/MWCNTs/polymer under simulated solar light irradiation, and (d) photocatalytic decolorization on CdS/MWCNTs/polymer in combination with H_2O_2 under simulated solar light irradiation. Experimental conditions: $[MO]_0=15$ mg L^{-1}; $[H_2O_2]_0=1.0$ mM; initial pH$=5.6$; photocatalyst dosage: 0.7 g L^{-1}.

Fig. 4. UV–visible spectral changes of MO solution during the photocatalytic decolorization by CdS/MWCNTs/polymer–H_2O_2 combination system under simulated solar light irradiation. Experimental conditions: $[MO]_0=15$ mg L^{-1}; $[H_2O_2]_0=1.0$ mM; initial pH$=5.6$; photocatalyst dosage: 0.7 g L^{-1}. Inset: the chemical structure of MO.

are 463.0 and 271.9 nm in the range of 200−600 nm, which is attributed to azo linkage and benzene, respectively. However, both two characteristic peaks were disappeared and no new peak appeared in analyzed wavelength range from 200 nm to 600 nm after 90 min under simulated solar light irradiation, indicated that MO has been completely decolorization and there were no reaction intermediates formed during the decolorization process.

The mechanism of highly efficient photocatalytic decolorization by CdS/MWCNTs/polymer–H_2O_2 system was given in Fig. 5. At first, electron/hole (e^-/h^+) pairs were photogenerated in CdS among CdS/MWCNTs/polymer composite photocatalyst under simulated solar light irradiation (Eq. (4)). Following, the photogenerated electrons transferred partly from CdS semiconductor to MWCNTs [24]. Another pathway
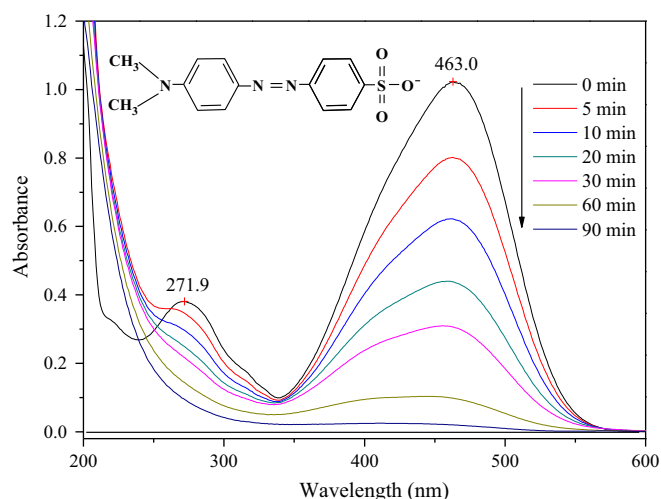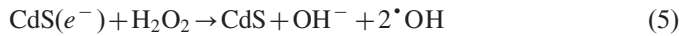
for the separation of photogenerated electron/hole pairs was that electrons on the CdS surface of photocatalyst were reacted with H_2O_2 to generate both OH$^-$ and $^\bullet$OH (Eq. (5)). In addition, O_2, acting as a scavenger, was reacted with the photogenerated electrons to generate superoxide radicals ($O_2^{\bullet-}$) (Eq. (6)), which would be further interacted with protons to yield $^\bullet$OOH radicals (Eq. (7)) [26,31]. At the same time, photogenerated holes (h^+) were also subsequently trapped by H_2O to yield $^\bullet$OH radicals (Eq. (8)). Effective separation of the photogenerated electron/hole pairs at the composite photocatalyst interface led to enhanced rates of photocatalytic decolorization. It is all known that these holes (h^+) and radicals ($^\bullet$OH and $^\bullet$OOH) are strong oxidizing agents, which can degrade and even mineralize completely all kinds of organic pollutants including azo dyes [26]. As a result, the combination of CdS/

MWCNTs/polymer with H_2O_2 can effectively increase the rate of photocatalytic decolorization and shorten the treatment time of dyes waste effluents.

$$CdS + hv \rightarrow CdS(e^-) + h^+ \tag{4}$$

$$CdS(e^-) + H_2O_2 \rightarrow CdS + OH^- + 2^\bullet OH \tag{5}$$

$$O_2 + e^- \rightarrow 2O_2^{\bullet -} \tag{6}$$

$$O_2^{\bullet -} + H^+ \rightarrow {}^\bullet OOH \tag{7}$$

$$h^+ + H_2O \rightarrow {}^\bullet OH + H^+ \tag{8}$$

3.3. Effect of photocatalyst dosage

In order to determine optimal dosage of photocatalyst, photocatalytic experiments were performed at 6.0 of initial pH, 15 mg L^{-1} of initial MO concentration and 1.0 mM of H_2O_2 concentration with different photocatalyst amounts. Fig. 6 showed the effect of photocatalyst dosage on decolorization of MO solution by CdS/MWCNTs/polymer–H_2O_2 system. Obviously, the decolorization percent of MO solution was found to increase with the increasing CdS/MWCNTs/polymer dosage up to about 0.7 g L^{-1}. However, a further increase of CdS/MWCNTs/polymer dosage from 0.7 g L^{-1} to

0.9 g L^{-1} had practically no effect on decolorization of MO solution.

To further investigate the decolorization kinetics of MO solution in CdS/MWCNTs/polymer–H_2O_2 system, a simplified Langmuir–Hinshelwood (L–H) kinetic model (Eqs. (9) and (10)), i.e. pseudo-first-order kinetic model, was applied to describe corresponding experimental data.

$$-\frac{dC}{dt} = k_{app}t \tag{9}$$

$$\text{i.e. } \ln\left(\frac{C_0}{C_i}\right) = k_{app}t \tag{10}$$

where t is the reaction time (min), k_{app} is the apparent pseudo-first-order reaction rate constant (min^{-1}), C_0 is the initial concentration of MO (mg L^{-1}), C_i is the instant concentration at reaction time t (mg L^{-1}). A plot of $\ln(C_0/C_i)$ versus t will yield a slope of k_{app}.

It was found that MO decolorization by CdS/MWCNTs/polymer–H_2O_2 system was followed the simplified Langmuir–Hinshelwood (L–H) kinetic model with high R^2 values (Fig. 6b). Under the same experimental conditions, the kinetic constant of MO decolorization was 0.0212 min^{-1}, 0.0308 min^{-1}, 0.03479 min^{-1}, 0.0426 min^{-1} and 0.0437 min^{-1} while photocatalyst dosage was 0.1, 0.3, 0.5, 0.7 and 0.9 g L^{-1}, respectively. The result suggested that at lower levels of photocatalyst dosage (0.1–0.7 g L^{-1}), increasing photocatalyst provided more reactive sites of photocatalysis resulting in the increase of the decolorization efficiency. However, further increase in photocatalyst dosage from 0.7 g L^{-1} to 0.9 g L^{-1} only brought the increase of kinetic constant (k_{app}) by 2.58%. Therefore, it is uneconomical for practical application when the amount of photocatalyst was above 0.7 g L^{-1}. Other previous researches have proven that aggregation of photocatalyst at higher concentration resulted in the decrease of photocatalytic decolorization [25]. As a result, 0.7 g L^{-1} of photocatalyst dosage was moderate for a given concentration of 15 mg L^{-1} of MO solution in CdS/MWCNTs/polymer–H_2O_2 system.
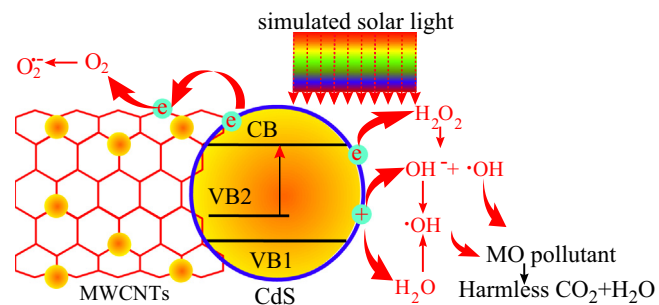

Fig. 5. Photocatalytic decolorization mechanism of CdS/MWCNTs/polymer–H_2O_2 combination system under simulated light irradiation.
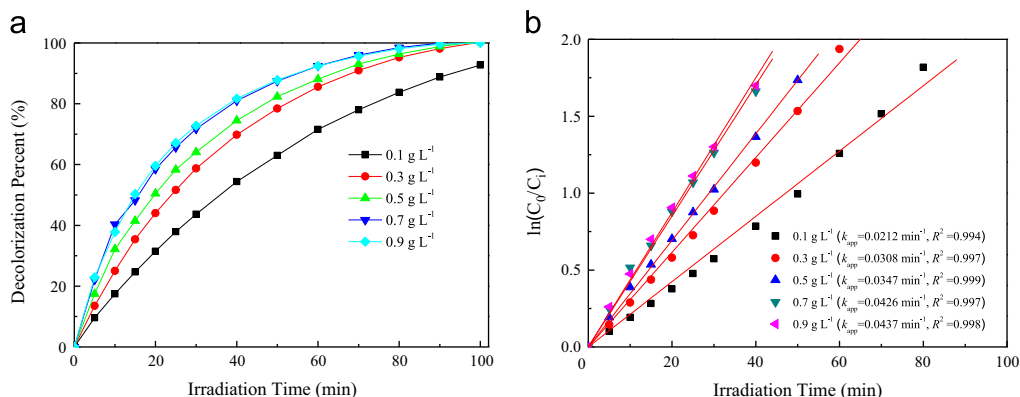

Fig. 6. Effect of photocatalyst dosage on decolorization percent (a) and apparent pseudo-first-order reaction rate constant (b) of MO solution in CdS/MWCNTs/polymer–H_2O_2 combination system under simulated solar light irradiation. Experimental conditions: [MO]$_0$ = 15 mg L^{-1}; [H$_2$O$_2$]$_0$ = 1.0 mM; initial pH = 6.0; photocatalyst dosage: 0.1–0.9 g L^{-1}.

3.4. Effect of H₂O₂ concentration

The effect of addition of H₂O₂ (0–1.5 mM) on photocatalytic oxidation has been investigated by applying five different H₂O₂ concentrations in the presence of MWCNTs/CdS/polymer (0.7 g L^{-1}). The results are shown in Fig. 7. The addition of H₂O₂ in the range of 0.0–1.0 mM increased decolorization percent from 70.5% to 98.5% after 90 min (Fig. 7a). The corresponding apparent pseudo-first-order reaction rate constant caused an obvious increase from 0.0158 min^{-1} to 0.0426 min^{-1}(Fig. 7b). However, further increase in H₂O₂ concentration from 1.0 to 1.5 mM, the decolorization of MO only increased by 0.10%. This phenomenon can be explained by two opposing effects with increasing the H₂O₂ concentration. On one hand, photodecomposition of H₂O₂ resulted in concentration enhance of ˙OH radicals in reaction solution [26]. H₂O₂ has been reported as an electron acceptor having a higher activity and efficiency in this role than oxygen for the photogenerated electrons in the conduction-band of photocatalyst (Eq. (5)).Therefore, more ˙OH radicals are available in solution to attack the aromatic rings of MO and the rate of

decolorization increased when the addition of H₂O₂ in the range of 0–1.0 mM. On the other hand, with further increase of H₂O₂ concentration, H₂O₂ acts as a hydroxyl radical quencher (Eqs. (11) and (12)) [32]. As a result, 1.0 mM of H₂O₂ concentration appears to be the optimal amount for the photocatalytic decolorization of MO solution (15 mg L^{-1}) in CdS/MWCNTs/polymer–H₂O₂ combination system.

$$H_2O_2 + {}^{\bullet}OH \rightarrow HO_2^{\bullet} + H_2O \tag{11}$$

$$HO_2^{\bullet} + {}^{\bullet}OH \rightarrow H_2O + O_2 \tag{12}$$

3.5. Effect of initial dye concentration

The effect of initial concentration of MO on the photocatalytic decolorization was investigated in the range of 5–30 mg L^{-1} since pollutant concentration is a very important parameter during water treatment. An increase in the initial concentration from 5 to 30 mg L^{-1} resulted in the decrease of the decolorization from 100% to 59.17% in 40 min. Similar results have been reported for the photocatalytic oxidation of
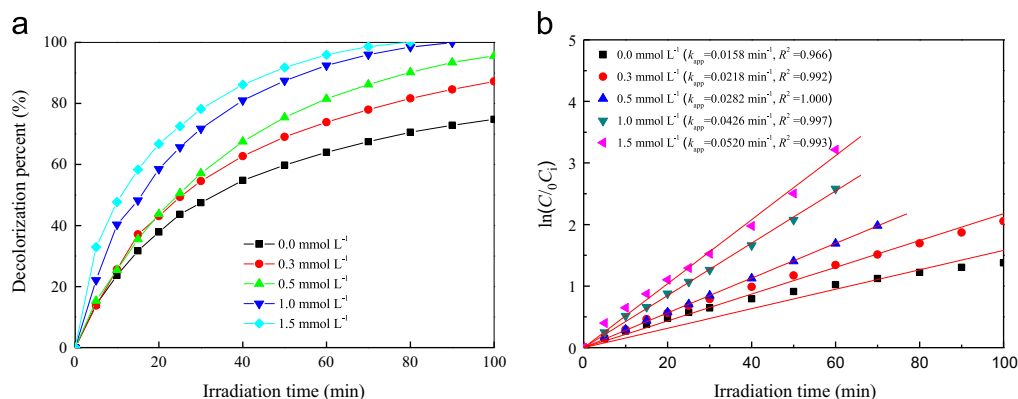

Fig. 7. Effect of H₂O₂ concentration on decolorization percent (a) and apparent pseudo-first-order reaction rate constant (b) of MO solution in CdS/MWCNTs/polymer–H₂O₂ combination system under simulated solar light irradiation. Experimental conditions: [MO]₀=15 mg L^{-1}; [H₂O₂]₀=0.0–1.5 mM; initial pH=6.0; photocatalyst dosage: 0.7 g L^{-1}.
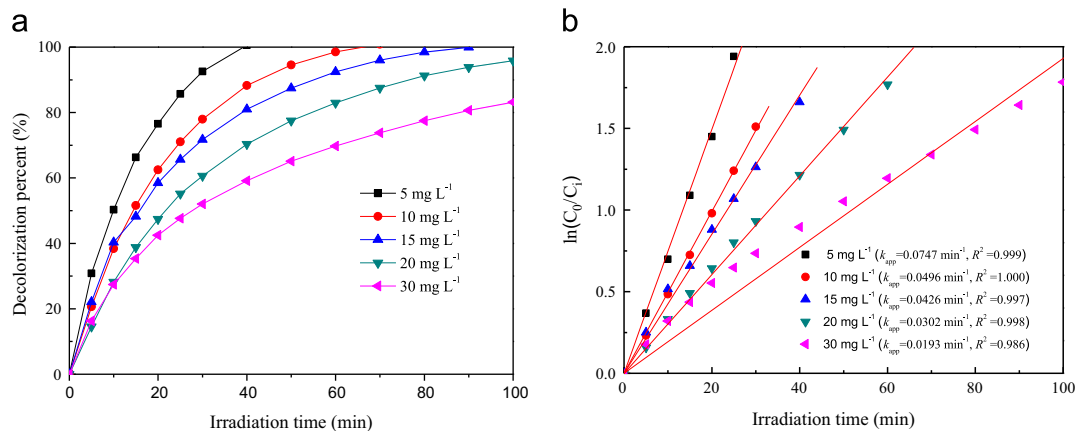

Fig. 8. Effect of initial dye concentration on decolorization percent (a) and apparent pseudo-first-order reaction rate constant (b) of MO solution in CdS/MWCNTs/polymer–H₂O₂ combination system under simulated solar light irradiation. Experimental conditions: [MO]₀=5–30 mg L^{-1}; [H₂O₂]₀=1.0 mM; initial pH=6.0; photocatalyst dosage: 0.7 g L^{-1}.

other dyes [33]. In addition, the time needed to achieve nearly complete decolorization increased expectedly from 40 min to 90 min with increasing initial concentration from 5 mg L^{-1} to 20 mg L^{-1} (Fig. 8a). For 15 mg L^{-1} of initial MO concentration, 99.9% of the azo dye solution was successfully decolorized after 90 min under simulated solar light irradiation. A linear plot between $\ln(C_0/C_i)$ and irradiation time has been observed and the result is shown in Fig. 8b. Obviously, the rate constant k_{app} decreased from 0.0747 min^{-1} to 0.0193 min^{-1} when the initial concentration of MO increased from 5 to 30 mg L^{-1}. For a certain amount of CdS/MWCNTs/polymer, the amount of active centers on the photocatalyst is finite while objective pollutant increases with increase of dye concentrations. The another important reason for the decrease of rate constant k_{app} with increasing MO concentrations is the fact that the penetration of photons entering into the MO solution decreases, so that an inner filter effect is induced and hence the MO solution becomes more and more impermeable to simulated solar light radiation [34].

3.6. Effect of pH

The effect of initial pH on photocatalytic decolorization of MO solution in CdS/MWCNTs/polymer–H$_2$O$_2$ system since the practical wastewater from textile industries usually has a wide range of pH values. Photocatalytic experiments were carried out under the same experimental conditions, but different initial pH in the range of 2.0–12.0. The corresponding result is shown in Fig. 9. The decolorization for MO dye was found to decrease with the increase in pH from 2.0 to 12.0 and highest efficiency was obtained at pH 2.0. At pH 2.0, pH 6.0, pH 8.0 and pH 12.0, the decolorization of MO solution was 100%, 87.43%, 72.37% and 23.98% in 50 min under simulated solar light irradiation, respectively (Fig. 9a). After 100 min irradiation, all MO solutions except pH 12.0 were decolored successfully excess 92.0%. As a result, a combination of CdS/MWCNTs/polymer and H$_2$O$_2$ (1.0 mM) was found to be highly efficient for photocatalytic decolorization of MO solution even at neutral pH values. From Fig. 9b, the kinetics rate

constant of photocatalytic decolorization was 0.0744 min^{-1}, 0.0426 min^{-1}, 0.0261 min^{-1}, and 0.0064 min^{-1} at initial pH 2.0, 6.0, 8.0 and 12.0, respectively. Therefore, the photocatalyitc process by CdS/MWCNTs/polymer–H$_2$O$_2$ system is more favorable in acidic medium. Similar observations have been observed by other researchers for some dyes [35,36].

3.7. Effect of coexisted anions

Existence of inorganic anions such as chloride (Cl$^-$), sulfate (SO$_4^{2-}$), carbonate (CO$_3^{2-}$), nitrate (NO$_3^-$), and phosphate (PO$_4^{3-}$) is considerably common in wastewaters, especially in dyeing effluent [37]. In this study, effects of various anions (Cl$^-$, H$_2$PO$_4^-$, NO$_3^-$, SO$_4^{2-}$, HPO$_4^{2-}$, CO$_3^{2-}$, and PO$_4^{3-}$) and combination between these anions on initial photocatalytic rate constants (k_{app}) and decolorization percent of MO solution by CdS/MWCNTs/polymer–H$_2$O$_2$ system were examined and the corresponding results are shown in Table 1. Obviously, the single additives (Cl$^-$, SO$_4^{2-}$, CO$_3^{2-}$, PO$_4^{3-}$) decreased both the photocatalytic rate and decolorization percent to some extent. Among all examined inorganic anions, PO$_4^{3-}$ showed the strongest effect followed by CO$_3^{2-}$, SO$_4^{2-}$, NO$_3^-$ and Cl$^-$. The inhibition effect on the photodegradation of pollutants has been recognized due to the occurrence of the competitive adsorption and less reactive radicals (such as SO$_2^{\bullet-}$) than $^{\bullet}$OH. There is not synergistic effect of photocatalytic decolorization in the presence of two coexisted anions (HPO$_4^{2-}$/H$_2$PO$_4^-$, PO$_4^{3-}$/CO$_3^{2-}$). These different effects of the anions highlight the necessary of testing various anions for practical application of CdS/MWCNTs/polymer–H$_2$O$_2$ system to degrade a pollutant.

3.8. Reuse of photocatalyst

Generally, the recovery of photocatalyst was one of the key steps to develop heterogeneous photocatalytic technology for practical application. The cycling runs in the photocatalytic decolorization of MO in CdS/MWCNTs/polymer–H$_2$O$_2$ system under simulated solar light were checked and are shown
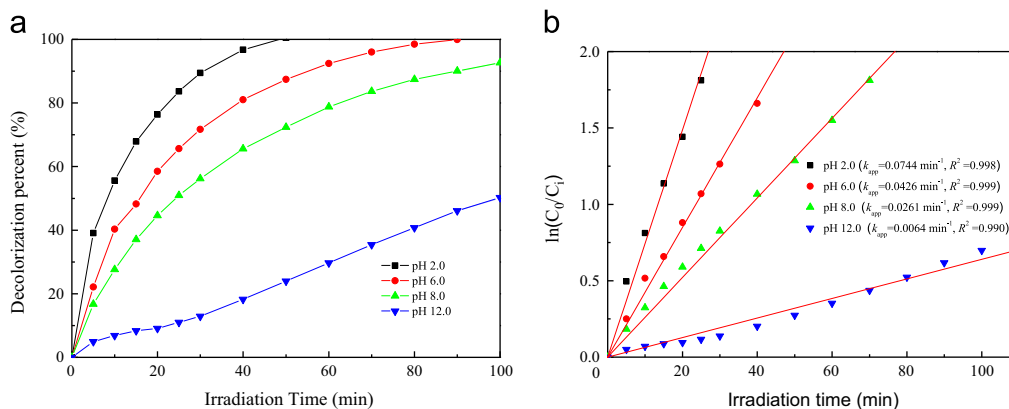

Fig. 9. Effect of pH on decolorization percent (a) and apparent pseudo-first-order reaction rate constant (b) of MO solution in CdS/MWCNTs/polymer–H$_2$O$_2$ combination system under simulated solar light irradiation. Experimental conditions: [MO]$_0$=15 mg L^{-1}; [H$_2$O$_2$]$_0$=1.0 mM; Initial pH (natural); photocatalyst dosage: 0.7 g L^{-1}.

Table 1

Effect of inorganic anions on MO decoloration CdS/MWCNTs/polymer–H_2O_2 system. Experimental conditions: $[MO]_0 = 15$ mg L^{-1}; $[H_2O_2] = 1.0$ mM; irradiation time: 90 min; photocatalyst dosage: 0.7 g L^{-1}.

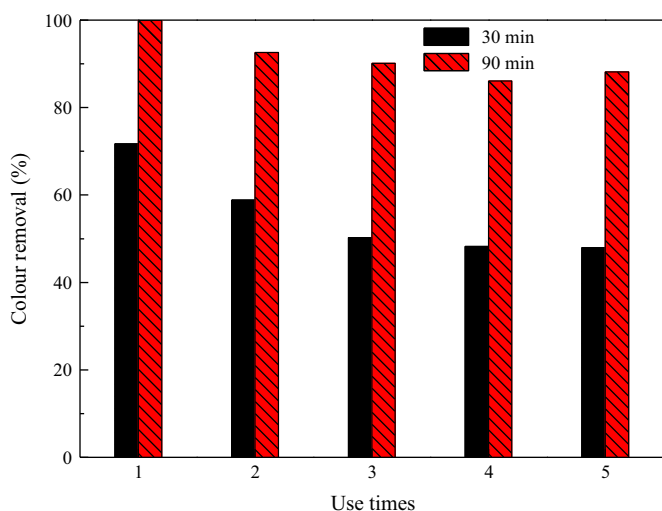| Anions	k_{app} (min^{-1})	% Decolorization (90 min)
–	0.042	99.92
Cl^-	0.025	91.13
$H_2PO_4^-$	0.024	87.45
NO_3^-	0.020	83.83
SO_4^{2-}	0.017	79.13
$HPO_4^{2-} + H_2PO_4^-$	0.016	75.60
HPO_4^{2-}	0.014	72.60
CO_3^{2-}	0.0114	65.13
$PO_4^{3-} + CO_3^{2-}$	0.0112	64.21
PO_4^{3-}	0.0106	61.41

Fig. 10. Cycling runs in the photocatalytic decolorization of MO in the presence of CdS/MWCNTs/polymer and H_2O_2. Experimental conditions: $[MO]_0 = 15$ mg L^{-1}; $[H_2O_2]_0 = 1.0$ mM; initial pH:6.0; photocatalyst dosage: 0.7 g L^{-1}.

in Fig. 10. The reused photocatalyst was filtered and then reused for the next experiment by adding the same dosage of H_2O_2. After five recycles, the decolorization efficiency decreased 11.7% approximately after 90 min irradiation. Thus, the combined CdS/MWCNTs/polymer–H_2O_2 (1.0 mM) process is promising method for practical application in water treatment.

4. Conclusions

In summary, a cadmium sulfide/multi-walled carbon nanotubes/polymer nanocomposite (CdS/MWCNTs/polymer) was fabricated by a facile precipitation process. Under simulated solar light irradiation, a combined CdS/MWCNTs/polymer–H_2O_2 (1.0 mM) process was found to be highly efficient for photocatalytic decolorization of a soluble azo dye, methyl orange (MO), even at neutral pH values. The decolorization of MO solution was strongly influenced by operational

parameters such as photocatalyst dosage, H_2O_2 concentration, pH and initial dye concentration and was followed the first-order kinetics with high R^2 values. 99.9% of azo dye solution was successfully decolorized after 90 min under simulated solar light irradiation with 15 mg L^{-1} of initial MO concentration, 1.0 mM of H_2O_2 concentration and 0.7 g L^{-1} of photocatalyst dosage. When the CdS/MWCNTs/polymer- H_2O_2 system was reused for the fifth time, the decolorization efficiency was still about 88.0% after 90 min under simulated solar light irradiation. As a result, this technique will potentially provide cheaper and cleaner means for treatment of a large volume of dyeing effluents since it increased substantially the efficiency of decolorization and could take full advantage of economical solar light.

References

[1] U. Bali, B. Karagözoğlu, Decolorization of remazol–turquoise blue G-133 and other dyes by Cu(II)/pyridine/H_2O_2 system, Dyes and Pigments 73 (2007) 133–140.

[2] K. Yu, S. Yang, C. Liu, H. Chen, H. Li, C. Sun, S.A. Boyd, Degradation of organic dyes via bismuth silver oxide initiated direct oxidation coupled with sodium bismuthate based visible light photocatalysis, Environmental Science and Technology 46 (13) (2012) 7318–7326.

[3] J. Fernández, J. Kiwi, J. Baeza, J. Freer, C. Lizama, H.D. Mansilla, Orange II photocatalysis on immobilised TiO_2 effect of the pH and H_2O_2, Applied Catalysis B 48 (2004) 205–211.

[4] V.K. Gupta, Suhas, Application of low-cost adsorbents for dye removal —a review, Journal of Environmental Management 90 (2009) 2313–2342.

[5] J.C. Garcia, J.L. Oliveira, A.E.C. Silva, C.C. Oliveira, J. Nozaki, N.E. de Souza, Comparative study of the degradation of real textile effluents by photocatalytic reactions involving UV/TiO_2/H_2O_2 and UV/Fe^{2+}/H_2O_2 systems, Journal of Hazardous Materials 147 (2007) 105–110.

[6] A. Geethakarthi, B.R. Phanikumar, Adsorption of reactive dyes from aqueous solutions by tannery sludge developed activated carbon: kinetic and equilibrium studies, International Journal of Environmental Science and Technology 8 (2011) 561–570.

[7] H.Y. Zhu, L. Xiao, R. Jiang, G.M. Zeng, L. Liu, Efficient decolorization of azo dye solution by visible light-induced photocatalytic process using SnO_2/ZnO heterojunction immobilized in chitosan matrix, Chemical Engineering Journal 172 (2011) 746–753.

[8] R. Jiang, H.Y. Zhu, J. Yao, Y.Q. Fu, Y.J. Guan, Chitosan hydrogel films as a template for mild synthesis of CdS quantum dots with highly efficient photocatalytic activity, Applied Surface Science 258 (2012) 3513–3518.

[9] U.G. Akpan, B.H. Hameed, Parameters affecting the photocatalytic degradation of dyes using TiO_2-based photocatalysts: a review, Journal of Hazardous Materials 170 (2009) 511–1282.

[10] Q. Li, B. Guo, J Yu, J. Ran, B. Zhang, H. Yan, J.R. Gong, Highly efficient visible-light-driven photocatalytic hydrogen production of CdS-cluster-decorated graphene nanosheets, Journal of the American Chemical Society 133 (2011) 10878–10884.

[11] M. Shang, W. Wang, S. Sun, J. Ren, L. Zhou, L. Zhang, Efficient visible light–induced photocatalytic degradation of contaminant by spindle–like

PANI/BiVO$_4$, Journal of Physical Chemistry C 113 (47) (2009) 20228–20233.

[12] R. Jiang, H.Y. Zhu, G.M. Zeng, L. Xiao, Y.J. Guan, Synergy of adsorption and visible light photocatalysis to decolour methyl orange by activated carbon/nanosized CdS/chitosan composite, Journal of Central South University of Technology 17 (2010) 1223–1229.

[13] L. Jia, D.H. Wang, Y.X. Huang, A.W. Xu, H.Q. Yu, Highly durable N-doped graphene/CdS nanocomposites with enhanced photocatalytic hydrogen evolution from water under visible light irradiation, Journal of Physical Chemistry C 115 (2011) 1466–11473.

[14] N. Zhang, Y. Zhang, X. Pan, X. Fu, S. Liu, Y.J. Xu, Assembly of CdS nanoparticles on the two-dimensional graphene scaffold as visible-light-driven photocatalyst for selective organic transformation under ambient conditions, Journal of Physical Chemistry C 115 (2011) 23501–23511.

[15] N. Soltani, E. Saion, M.Z. Hussein, M. Erfani, A. Abedini, G. Bahmanrokh, M. Navasery, P. Vaziri, Visible light-induced degradation of methylene blue in the presence of photocatalytic ZnS and CdS nanoparticles, International Journal of Molecular Sciences 13 (2012) 12242–12258.

[16] H.Y. Zhu, R. Jiang, L. Xiao, Y.H. Chang, Y.J. Guan, X.D. Li, G. M. Zeng, Photocatalytic decolorization and degradation of congo red on innovative crosslinked chitosan/nano-CdS composite catalyst under visible light irradiation, Journal of Hazardous Materials 169 (2009) 933–994.

[17] J.L. Wang, L.J. XU, Advanced oxidation processes for wastewater treatment: formation of hydroxyl radical and application, Critical Reviews in Environmental Science and Technology 42 (2012) 251–325.

[18] X.B. Hu, Y.H. Deng, Z.Q. Gao, B.Z. Liu, C. Sun, Transformation and reduction of androgenic activity of 17-methyltestosterone in Fe$_3$O$_4$/MWCNTs–H$_2$O$_2$ system, Applied Catalysis B 127 (2012) 167–174.

[19] J.L. Gong, B. Wang, G.M. Zeng, C.P. Yang, C.G. Niu, Q.Y. Niu, W. J. Zhou, Y. Liang, Removal of cationic dyes from aqueous solution using magnetic multi-wall carbon nanotube nanocomposite as adsorbent, Journal of Hazardous Materials 164 (2009) 1517–1522.

[20] S. Qu, H. Fei, S. Yu, G. Chen, J. Kong, Magnetic removal of dyes from aqueous solution using multi-walled carbon nanotubes filled with Fe$_2$O$_3$ particles, Journal of Hazardous Materials 160 (2008) 643–647.

[21] C.S. Li, Y.P. Tang, B.N. Kang, B.S. Wang, F. Zhou, Q. Ma, J. Xiao, D. Z. Wang, J. Liang, Photocatalytic degradating methyl orange in water phase by UV-irradiated CdS carried by carbon nanotubes, Science in China Series E: Technological Sciences 50 (2007) 279–289.

[22] Y. Liu, L. Gao, In situ coating multiwalled carbon nanotubes with CdS nanoparticles, Materials Chemistry and Physics 91 (2005) 365–369.

[23] X.W. Wei, X.J. Song, J. Xu, Y.H. Ni, P. Zhang, Coating multi-walled carbon nanotubes with metal sulfides, Materials Chemistry and Physics 92 (2005) 159–163.

[24] K. Ouyang, S. Xie, X. Ma, Photocatalytic activity of TiO$_2$ supported on multi-walled carbon nanotubes under simulated solar irradiation, Ceramics International 39 (2013) 7531–7536, http://dx.doi.org/10.1016/j.ceramint.2013.03.004.

[25] H.Y. Zhu, R. Jiang, Y.J. Guan, Y.Q. Fu, L. Xiao, G.M. Zeng, Effect of key operational factors on decolourization of methyl orange during H$_2$O$_2$ assisted nanosized CdS/TiO$_2$/polymer composite thin films under simulated solar light irradiation, Separation and Purification Technology 74 (2010) 187–194.

[26] M. Harir, A. Gaspar, B. Kanawati, A. Fekete, M. Frommberger, D. Martens, A. Kettrup, M. El Azzouzi, P. Schmitt–Kopplin, Photocatalytic reactions of imazamox at TiO$_2$, H$_2$O$_2$ and TiO$_2$/H$_2$O$_2$ in water interfaces: kinetic and photoproducts study,, Applied Catalysis B 84 (2008) 524–532.

[27] H. Liu, Y.M. Du, J.H. Yang, H.Y. Zhu, Structural characterization and antimicrobial activity of chitosan/betaine derivative complex, Carbohydrate Polymers 55 (2004) 291–297.

[28] Y Hu, Y Du, J Yang, Y Tang, J Li, X Wang, Self-aggregation and antibacterial activity of N-acylated chitosan, Polymer 48 (2007) 3098–3106.

[29] H. Cao, B. Wei, Y. Wang, Y. Li, M. Zhu, Synthesis of a carbon nanotubes magnetic composite by chemical precipitation–hydrothermal process, Journal of the Chinese Ceramic Society 37 (2009) 1772–1776.

[30] N.M. Mahmoodi, M. Arami, N.Y. Limaee, N.S. Tabrizi, Kinetics of heterogeneous photocatalytic degradation of reactive dyes in an immobilized TiO$_2$ photocatalytic reactor, Journal of Colloid and Interface Science 295 (2006) 159–164.

[31] X. Zhao, Y. Zhu, Synergetic degradation of rhodamine B at a porous ZnWO$_4$ film electrode by combined electro-oxidation and photocatalysis, Environmental Science and Technology 40 (2006) 3367–3372.

[32] M. Muruganandham, M. Swaminathan, Advanced oxidative decolourisation of reactive yellow 14 azo dye by UV/TiO$_2$, UV/H$_2$O$_2$, UV/H$_2$O$_2$/Fe^{2+} processes—a comparative study, Separation and Purification Technology 48 (2006) 297–303.

[33] M. Muruganandham, N. Shobana, M. Swaminathan, Optimization of solar photocatalytic degradation conditions of reactive yellow 14 azo dye in aqueous TiO$_2$, Journal of Molecular Catalysis A 246 (2006) 154–161.

[34] N. Daneshvara, M.A. Behnajadyb, M.K.A. Mohammadi, M.S.S. Dorraji, UV/H$_2$O$_2$ treatment of Rhodamine B in aqueous solution: influence of operational parameters and kinetic modeling, Desalination 230 (2008) 16–26.

[35] M. Saquib, M. Abu Tariq, M.M. Haque, M. Muneer, Photocatalytic degradation of disperse blue 1 using UV/TiO$_2$/H$_2$O$_2$ process, Journal of Environmental Management 88 (2008) 300–306.

[36] G. Li, X.S. Zhao, M.B. Ray, Advanced oxidation of orange II using TiO$_2$ supported on porous adsorbents: the role of pH, H$_2$O$_2$ and O$_3$, Separation and Purification Technology 55 (2007) 91–97.

[37] H.C. Liang, X.Z. Li, Y.H. Yang, K.H. Sze, Effects of dissolved oxygen, pH, and anions on the 2,3-dichlorophenol degradation by photocatalytic reaction with anodic TiO$_2$ nanotube films, Chemosphere 73 (2008) 805–812.